Type IV Wind Turbine System Impedance Modelling for Harmonic Analysis On the Use of a Double Synchronous Reference Frame and Notch Filter

Beloqui Larumbe, Lucia; Qin, Zian; Bauer, Pavol

Publication date
2018

Document Version
Final published version

Published in
Digital Proceedings of the 17th International Workshop on Large-Scale Integration of Wind Power into Power Systems as well as on Transmission Networks for Offshore Wind Power Plants

Type IV Wind Turbine System Impedance Modelling for Harmonic Analysis

On the Use of a Double Synchronous Reference Frame and Notch Filter

Lucia Beloqui Larumbe, Zian Qin, Pavol Bauer
Electrical Sustainable Energy Department
Delft University of Technology
Delft, The Netherlands
L.BeloquiLarumbe@tudelft.nl

***Abstract*—Several efforts are being done nowadays to improve the modelling of Wind Turbine Systems (WTSs) for harmonic analysis in Offshore Wind Power Plants (OWPPs). Due to the high influence of the different control structures in the Power Electronic Converters (PECs) on the dynamic response of a WTS, each structure needs to be modelled specifically. In the case of this paper, the control approach under study is a double Synchronous Reference Frame. The main focus lies on the correct modelling of one of the main elements of this structure: the notch filter tuned at twice the fundamental frequency. It has been shown that this filter has indeed a notable effect on shaping the frequency response of a WTS, however, the modelling of this filter in the αβ frame in previous works was inaccurate. This inaccuracy and its implications are detailed in this paper. Simulation results confirm the theoretical findings.**

Keywords: wind turbine harmonic model; offshore wind power plant; notch filter; double synchronous reference frame

I. INTRODUCTION

Several efforts are being done nowadays to improve and standardize the harmonic assessment in Offshore Wind Power Plants (OWPPs) [1]. Apart from improved harmonic propagation studies or more efficient Wind Turbine (WT) measurement campaigns, one of the main focuses lies on the accurate modelling of Wind Turbines [2].

The main challenges lie in obtaining models that are able to represent the harmonic emission of the Wind Turbine Systems (WTSs, defined as the WT with the power electronic conversion stage) and at the same time the interactions with the external electric network and other converters. In this sense, it has already been shown that the control loops in the Power Electronic Converters (PECs) have a considerable impact on the harmonic response of a WTS [3]-[4]. However, it has not yet been addressed thoroughly which of the control parameters (e.g. Phase-Locked Loop (PLL) bandwidth, current loop stability margin) are most influential and in what frequency range.

This paper is focused on the impedance part of the harmonic model of a WTS (typically composed on a frequency-dependent current source and a parallel impedance [5]- [6]). In this paper, a double Synchronous Reference Frame (SRF) is going to be considered instead of the typically assumed single SRF structure (i.e., it is going to be considered that the positive and negative sequences are controlled separately instead of both of them going through the same dq frame). The single SRF structure is simpler and *a priori* easier to analyze than the double SRF, however, the double SRF might become more widespread in state-of-the-art WTSs due to its superior dynamic performance under unbalanced grid conditions [7]. Indeed, the double SRF has been considered in the impedance modelling of WTS before (e.g. [4]), but the difference between modelling this structure and a single SRF has not been explicitly shown before.

With this objective in mind, this paper provides the first step for the purpose, which is the modelling of one specific element that is used in the double SRF structure that is not typically used in the single SRF structure: the notch filter that is used for separating the positive and negative sequence signals. The inclusion or disregard of this notch filter is very important because, as shown in [4], this filter can have a big influence on the shaping of the WTS output impedance and such of the OWPP. However, the modelling procedure for the notch filter followed in [4] ignores the cross-couplings that this element creates in the αβ frame, which leads to a wrong calculation of the WTS impedance in the lower frequency range.

The main contribution of this paper is, thus, to show the importance of these cross couplings in the notch filter and to explain how to model them. Simulation results uphold the theoretical model proposed in this paper.

Future works will use this first step (i.e. the notch filter model) and will explain in detail the procedure for modelling the impedance of the complete double SRF. Despite this, still in this paper the resultant impedance of a Type IV WTS with double SRF in which the notch filter is calculated with the model proposed in [4] will be compared to such impedance but with the notch filter calculated as proposed in this paper. The considerable differences in these impedances highlights the importance of a proper modelling of the notch filter.

With this purpose, Section II describes the WTS under study. In Section III, the theoretical explanation on how to properly model the notch filter is addressed. In Section IV, simulations results are shown. Section V briefly shows the impact of the different notch filter models in the output impedance of a WTS. Conclusions are drawn in Section VI.

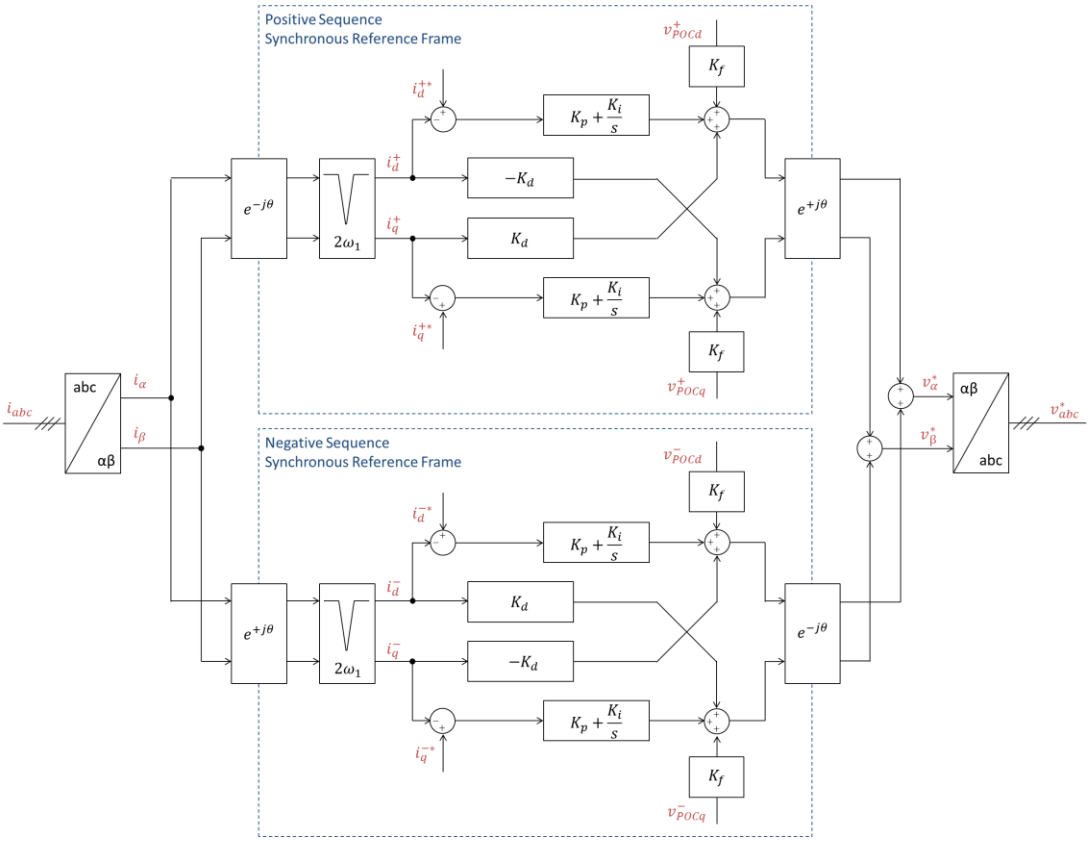

Figure 2. Schematic of the control structure in a double Synchronous Reference Frame

II. Wind Turbine System Description

In this paper, the Type IV WT was selected as this is the common choice for offshore applications due to its excellent dynamic response [3]. The power electronic stage consists of a back-to-back full converter as shown in Fig. 1.

The DC voltage is considered constant in this study, so the dynamics of both converters can be decoupled. The focus of this article is on the grid-side converter as this is the one facing the OWPP. The main parameters of this PEC, a two-level VSC, can be found in TABLE I. The values were chosen in order to approximate the situation in a real offshore WTS. The constant-DC voltage approximation implies the omission of the DC voltage control loop.

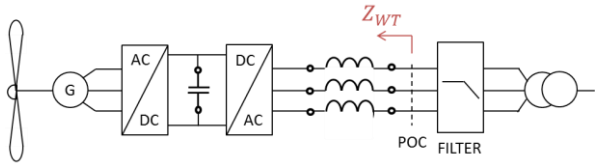

Figure 1. Schematic of a Type IV Wind Turbine

A. Control Structure

The current control loop might be implemented in different ways, but based on the literature it was decided to use a rotating dq reference frame synchronized with the power system frequency by a Phase-Locked Loop (PLL).

In order to improve dynamic performance, especially in the case of voltage unbalances, a common procedure is to control the positive and negative sequences separately and simultaneously [7]. In order to do this, the positive sequence is controlled in a positive sequence synchronous reference frame (SRF) in which there is a PI. Additionally, the negative sequence is controlled in a negative sequence SRF with another PI. The key point is that in the positive SRF, a positive sequence signal appears as a DC signal, while a negative sequence appears as an AC signal at twice the fundamental frequency. Thus, it is very easy to filter the negative sequence in the positive sequence frame if a notch filter is tuned at a $2f_1$ (with f_1 being the fundamental frequency, 50Hz in this paper). Similarly can be done in the negative SRF. The formula for the notch filter and a discussion on its effects will be provided later in Section III. The schematic of this control structure is shown in Fig. 2.

Note that, for the case of this specific paper, the focus is exclusively on the notch filter depicted in Fig. 2. The rest of the elements described in here will be used in order to calculate the WTS impedance at the end of this paper, although the exact procedure for this final impedance calculation will be shown in a follow-up paper.

The formula for the PI controller can be found in (1). The values chosen for this PI are shown in TABLE II. The values have been chosen with $K_i=K_pR_L/L$ in order to compensate for the pole in the plant (where L is the output filter inductor and R_L its resistance). K_p was selected to obtain a bandwidth BW=200Hz (10 times lower than the switching frequency F_{sw}=2kHz).

TABLE I. MAIN PARAMETERS OF THE GRID-SIDE POWER ELECTRONIC CONVERTER

	Description	Value	Unit
V_{dc}	DC Voltage	1200	V
V_{ac}	Line-to-line AC Voltage	690	V
P_{rated}	Rated Power	4.2	MW
L	Output Inductor	48.71 (0.15)	μH (p.u.)

	Description	Value	Unit
R_L	Resistance of Output Inductor	30 (0.15/5)	mΩ (p.u.)
	Operating Point		
I_1	Output Current	4.97 (nominal)	kA
ϕ_{i1}	Angle difference between Current and Phase Voltage	0	degrees

TABLE II. MAIN PARAMETERS OF THE STUDIED CONTROL LOOPS

	Description	Value	Unit
F_s	Sampling Frequency	4000	Hz
K_d	Current Coupling Compensation Gain	$L\omega_1$=0.0153	Ω
K_f	Voltage Feedforward Gain	0	V/V
	Current Control		
K_p	Proportional Constant PI	0.062	Ω
K_i	Integral Constant PI	37.7	Ω/s
BW_i	Current Control Bandwidth	200	Hz

	Description	Value	Unit
	Phase-Locked Loop		
$K_{p\text{-}pll}$	Proportional Constant PI	0.3	rad/s
$K_{i\text{-}pll}$	Integral Constant PI	12	rad/s^2
BW_{pll}	PLL Bandwidth	30	Hz
	Filters in the Sensors		
ω_{fi}	Cut-off freq. of filter current sensor	2π 2000	rad/s
ω_{fv}	Cut-off freq. of filter voltage sensor	2π 2000	rad/s

$$H_i(s) = K_p + \frac{K_i}{s} \tag{1}$$

Further, the current control includes a current coupling compensation gain (K_d) which is selected as Lω and a voltage feedforward gain (K_f). In this case, the voltage feedforward has not been included (K_f=0) for simplification.

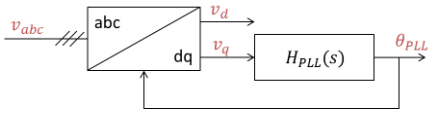

Figure 3. Synchronous Reference Frame PLL (SRF-PLL)

The PLL under study is a basic SRF-PLL as depicted in Fig. 3. The PLL compensator ($H_{PLL}(s)$) has been chosen to be a simple PI with an additional integrator as in (2). The closed-loop transfer function of the PLL is given by (3) [8].

$$H_{PLL}(s) = \left(K_p + \frac{K_i}{s}\right)\frac{1}{s} \tag{2}$$

$$T_{PLL}(s) = \frac{H_{PLL}(s)}{1 + V_1 H_{PLL}(s)} \tag{3}$$

Where V_1 is the amplitude of the AC output phase voltage. In [8] T_{PLL} is also multiplied in the numerator by V_1. However, this is due to the fact that the author assumes that the signal values in the control blocks will be in p.u.

Finally, in (4) and (5), $G_i(s)$ represents the filter in the current measuring system and the sampling delay, and $G_v(s)$ represents the same for the AC voltage signal (used in the feedforward voltage and as an input to the PLL).

$$G_i(s) = e^{-s1.5T_s}\frac{\omega_{fi}^2}{s^2 + 2\xi\omega_{fi}s + \omega_{fi}^2} \tag{4}$$

$$G_v(s) = e^{-s1.5T_s}\frac{\omega_{fv}^2}{s^2 + 2\xi\omega_{fv}s + \omega_{fv}^2} \tag{5}$$

Where T_s is the sampling time (T_s=1/F_s with F_s=2F_{sw} as in TABLE II.), ξ is the damping factor and is selected equal to 1, and ω_{fi} and ω_{fv} are the cut-off frequencies of the filter of the current and voltage sensors, respectively.

Note on Fig. 1 that the objective is to calculate the impedance of the WTS (Z_{WT}) up until and including the output inductor. The possible additional filter stages can be added *a posteriori* to the impedance of the converter by linear circuit theory.

III. THEORETICAL MODEL OF THE NOTCH FILTER

A typical notch filter is shown in (6).

$$H_n(s) = \frac{s^2 + \left(\frac{\omega_n}{Q_n}\right)s + \omega_n^2}{s^2 + \left(\frac{\omega_n}{Q_d}\right)s + \omega_n^2} \tag{6}$$

Where ω_n is the angular frequency at which the filter is tuned and Q_n and Q_d are constants that need to be tuned according to the application [4]. The parameters chosen for this filter are Q_n=10/sqrt(2), Q_d=2/sqrt(2) and ω_n=2ω_1 as in [4]. The response of the filter can be seen in Fig. 4.

As implied in Fig 2, the notch filter is applied to both dq channels separately, as in (7).

$$\begin{bmatrix} i_d \\ i_q \end{bmatrix} = \underbrace{\begin{bmatrix} H_n(s) & 0 \\ 0 & H_n(s) \end{bmatrix}}_{H_{n\ dq}^{m}(s)} \begin{bmatrix} i_{d\_unfiltered} \\ i_{q\_unfiltered} \end{bmatrix} \tag{7}$$

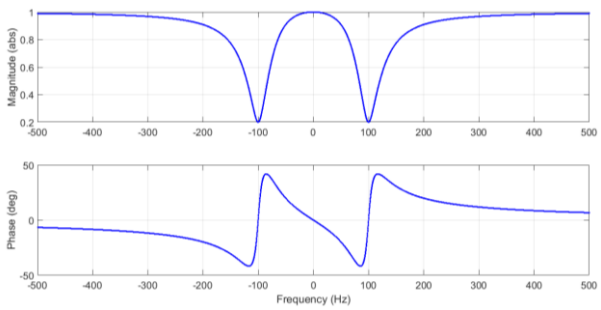

Figure 4. Notch filter in the dq frame (as in (11))

$H_n{}^m{}_{dq}(s)$ is a transfer matrix (m is upper-index for transfer matrix) in de dq frame (dq sub-index). If this transfer matrix is to be translated into the αβ frame, it is very useful to represent it as a complex transfer function because the translation is just a frequency shift (for basic theory on transfer matrices and complex transfer functions see [9]).

Note that $H_n{}^m{}_{dq}(s)$ not only is symmetrical (the diagonal terms are equal and the cross-diagonal terms have opposite signs) but also that the cross-diagonal terms are zero. The first characteristic implies that, when representing $H_n{}^m{}_{dq}(s)$ with complex transfer functions, only one transfer function is needed, and the second characteristic that the complex transfer function will actually have a zero imaginary part.

More specifically, if the element (1,1) in $H_n{}^m{}_{dq}(s)$ is called $G_{dd}(s)$, the element (1,2) is $-G_{qd}(s)$, the element (2,1) is $G_{dq}(s)$ and the element (2,2) is $G_{qq}(s)$, we can rename $G_{dd}(s)= G_{qq}(s)=G_d(s)$ and $G_{dq}(s)= G_{qd}(s)=G_q(s)$. In order to transform it into a complex transfer function $H_n{}^c{}_{dq}(s)$ (c upper-index) then (8) applies.

$$H^c_{n\,dq}(s) = G_d(s) + jG_q(s) = H_n(s) + j0 \tag{8}$$

Thus, due to the special characteristics of (7), the complex transfer function is simply $H_n(s)$. Now, in order to translate this complex transfer function into the alpha beta frame, the only thing to do is a frequency shift as in (9) [9].

$$H^c_{n\,\alpha\beta}(s) = H^c_{n\,dq}(s - j\omega_1) = H_n(s - j\omega_1) = \\ = \frac{(s - j\omega_1)^2 + \left(\frac{\omega_n}{Q_n}\right)(s - j\omega_1) + \omega_n^2}{(s - j\omega_1)^2 + \left(\frac{\omega_n}{Q_d}\right)(s - j\omega_1) + \omega_n^2} \tag{9}$$

Equation (9) shows a complex transfer function $H_n(s\text{-}j\omega_1)$ that is the notch filter in the αβ frame. Note that now, the imaginary part is non-zero due to the frequency shift.

In order to understand what this means more intuitively, it is useful to translate this into a transfer matrix again (like (12) but in the αβ frame). This transfer matrix will have the following elements: (1,1) is called $G_{\alpha\alpha}(s)$, (1,2) is $-G_{\beta\alpha}(s)$, (2,1) is $G_{\alpha\beta}(s)$ and (2,2) is $G_{\beta\beta}(s)$. As the filter is represented by only one complex transfer function, it is known that the corresponding transfer matrix is symmetric, thus: $G_{\alpha\alpha}(s)= G_{\beta\beta}(s)=G_\alpha(s)$ and $G_{\alpha\beta}(s)= G_{\beta\alpha}(s)=G_\beta(s)$. In order to find $G_\alpha(s)$ and $G_\beta(s)$, (10) and (11) are applicable [9].

$$G_\alpha(s) = \frac{H^c_{n\,\alpha\beta}(s) + H^{c*}_{n\,\alpha\beta}(s)}{2} \tag{10}$$

$$G_\beta(s) = \frac{H^c_{n\,\alpha\beta}(s) - H^{c*}_{n\,\alpha\beta}(s)}{2j} \tag{11}$$

Where the upper-index * in (10) and (11) means conjugate. In this case, the conjugate would be given by (12).

$$H^{c*}_{n\,\alpha\beta}(s) = \frac{(s + j\omega_1)^2 + \left(\frac{\omega_n}{Q_n}\right)(s + j\omega_1) + \omega_n^2}{(s + j\omega_1)^2 + \left(\frac{\omega_n}{Q_d}\right)(s + j\omega_1) + \omega_n^2} \tag{12}$$

Thus, with (10), (11) and (12) the transfer matrix in the αβ frame can be obtained as in (13).

$$\begin{bmatrix} i_\alpha \\ i_\beta \end{bmatrix} = \underbrace{\begin{bmatrix} G_\alpha(s) & -G_\beta(s) \\ G_\beta(s) & G_\alpha(s) \end{bmatrix}}_{H^m_{n\ \alpha\beta}(s)} \begin{bmatrix} i_{\alpha\_unfiltered} \\ i_{\beta\_unfiltered} \end{bmatrix} \tag{13}$$

where $G_\alpha(s)$ and $G_\beta(s)$ are the real and the imaginary part of $H_n{}^c{}_{\alpha\beta}(s)$ (shown in (18)), as it is indicated in (14).

$$H^c_{n\,\alpha\beta}(s) = G_\alpha(s) + jG_\beta(s) \tag{14}$$

This is the same procedure followed in [4]. The difference is that in [4] the cross-diagonal terms in the αβ transfer matrix (that is to say, $G_\beta(s)$) are assumed to be irrelevant, and the notch filter in the αβ frame is simply modelled as $G_\alpha(s)$. That is to say, in the complex transfer function representation, the imaginary part is neglected.

Fig. 6 shows the notch filter in the αβ frame (that is to say, $H_n(s\text{-}j\omega_1)$ as in (14)), its real part $G_\alpha(s)$ and its imaginary part $G_\beta(s)$. As it can be seen, $G_\beta(s)$ a priori might seem insignificant because of its low magnitude in comparison to $G_\alpha(s)$. However, the effect of $G_\beta(s)$ is actually quite significant, as shown by the big difference in between $H_n(s\text{-}j\omega_1)$ and $G_\alpha(s)$, in both the magnitude and phase plots.

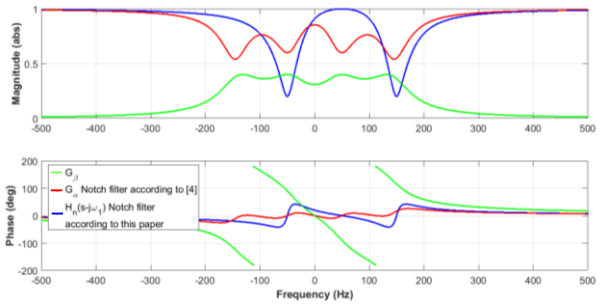

Figure 5. Notch filter in the αβ frame ($H_n(s\text{-}j\omega_1)$ as in (14)), its real part $G_\alpha(s)$ and its imaginary part $G_\beta(s)$. Note the frequency shift of $H_n(s\text{-}j\omega_1)$, in blue, with respect to Fig. 4.

Thus, it is considered in this paper that (9) is the correct representation of the notch filter, which indeed makes sense because as expected, it clearly filters the negative sequence component at -50 Hz while having magnitude 1 and phase 0 degrees for the positive sequence at 50 Hz.

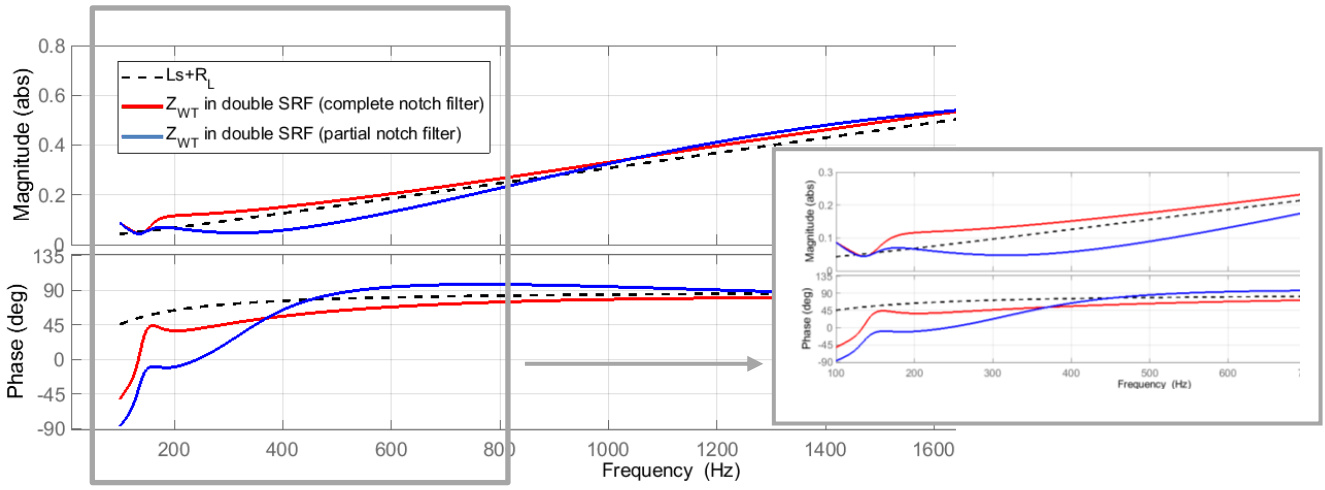

Figure 8. Impedance of a Type IV WT considering a double Synchronous Reference Frame with a complete notch filter as in (9) (red), and the same but with a partial notch filter (ignoring the couplings) (blue)

IV. Simulation Results

In order to uphold this analytic analysis, several simulations where carried out in Simulink. The system simulated is shown schematically in Fig. 6

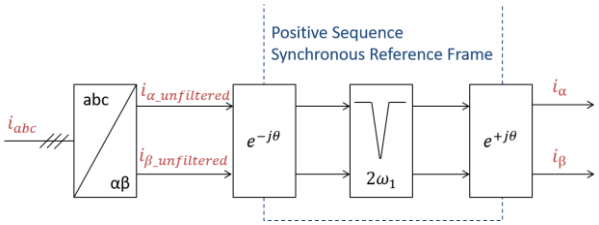

Figure 6. Schematic of the simulated system

The objective was to calculate the complex transfer function between the signal before the filter ($i_{\alpha\beta unfiltered}$) and the signal after the filter ($i_{\alpha\beta}$) in the αβ frame to check the validity of (9). In order to do so, the three phase signal i_{abc} was varied over a frequency range, both in the positive and negative sequences. Subsequently, $H_n{}^c{}_{\alpha\beta}(s) = H_n(s\text{-}j\omega_1)$ was calculated according to (15).

$$H^c_{n\,\alpha\beta}(s) = \frac{i_\alpha + j i_\beta}{i_{\alpha\_unfiltered} + j i_{\beta\_unfiltered}} \qquad (15)$$

The results of this procedure are shown in Fig. 7 As it can be seen, the theoretical formula shown in (9) accurately matches the simulation results.

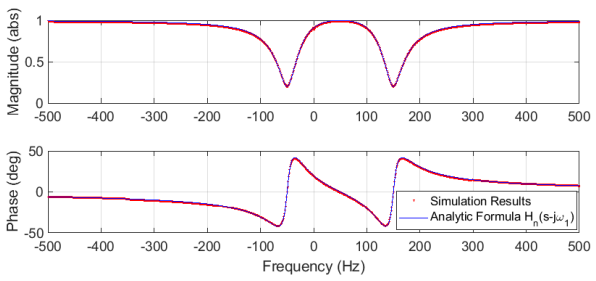

Figure 7. Comparison of simulation results (red) with the theoretical model (blue). Note: the blue curve is the same as in Fig. 5.

V. Impact of the Notch Filter on the Harmonic Impedance of a Type IV WTS

In Fig. 8 it can be seen the curve of the output filter inductor ($Ls+R_L$), the impedance with a double SRF in which the notch filter has been calculated with (9) and the impedance with a double SRF but with the notch filter only partially included (only the real part, as done in [4]). Firstly, in this figure it is shown the considerable effect of the notch filter in shaping the output impedance of a WTS in the low frequency range. Secondly, the figure highlights also the importance of including both the real and the imaginary parts of the notch filter complex transfer function. That is to say, to consider both $G_\alpha(s)$ and $G_\beta(s)$ in (14) or, in other words, to not neglect the cross-couplings of the notch filter when transferred into the αβ frame.

VI. Conclusions

With the objective of analytically calculating the harmonic impedance of a WTS in the case of the use of a double SRF, this paper has provided the first step for the purpose: the modelling of the notch filter tuned at twice the fundamental frequency.

The theoretical analysis behind the correct modelling of this filter has been provided using transfer matrices and complex transfer functions transformations, and the final model has been validated with simulations.

The importance of including the couplings that the notch filter creates when transferred into the αβ frame has been shown by highlighting the great influence of these couplings in the final shaping of the output impedance of a Type IV WTS in the low frequency range.

References

[1] B. Andresen, L. Christensen, I. Skrypalle, Ł. H. Kocewiak, F. Santjer, "Overview, Status and Outline of the New Standards Series - IEC 61400 -21 – Measurement and Assessment of Electrical Characteristics - Part I - Wind Turbines and Part II - Wind Power Plants," in Proc. The 14th International Workshop on Large-Scale Integration of Wind Power into Power Systems as well as Transmission Networks for Offshore Wind Farms, Energynautics GmbH, 20-22 October 2015, Brussels, Belgium.

[2] Ł. H. Kocewiak, C. Álvarez, P. Muszynski, J. Cassoli, L. Shuai, "Wind Turbine Harmonic Model and Its Application – Overview, Status and Outline of the New IEC Technical Report," in Proc. The 14th International Workshop on Large-Scale Integration of Wind

Power into Power Systems as well as Transmission Networks for Offshore Wind Farms, Energynautics GmbH, 20-22 October 2015, Brussels, Belgium.

[3] L. Shuai, Ł. H. Kocewiak, K. Høj Jensen, “Application of Type 4 Wind Turbine Harmonic Model for Wind Power Plant Harmonic Study,” in Proc. The 15th International Workshop on Large-Scale Integration of Wind Power into Power Systems as well as Transmission Networks for Offshore Wind Farms, Energynautics GmbH, 15-17 November 2016, Vienna, Austria.

[4] L. H. Kocewiak, J. Hjerrild and C. L. Bak, "Wind turbine converter control interaction with complex wind farm systems," in IET Renewable Power Generation, vol. 7, no. 4, pp. 380-389, July 2013.

[5] J. Sun, "Impedance-Based Stability Criterion for Grid-Connected Inverters," in IEEE Transactions on Power Electronics, vol. 26, no. 11, pp. 3075-3078, Nov. 2011.

[6] L. Beloqui Larumbe, Z. Qin, P. Bauer, “Introduction to the Analysis of Harmonics and Resonances in Large Offshore Wind Power Plants”, IEEE-PEMC 2018- 18th International Conference on Power Electronics and Motion Control, Budapest, Hungary, 2018.

[7] Hong-Seok Song and Kwanghee Nam, "Dual current control scheme for PWM converter under unbalanced input voltage conditions," in IEEE Transactions on Industrial Electronics, vol. 46, no. 5, pp. 953-959, Oct 1999.

[8] M. Cespedes and J. Sun, "Impedance Modeling and Analysis of Grid-Connected Voltage-Source Converters," in IEEE Transactions on Power Electronics, vol. 29, no. 3, pp. 1254-1261, March 2014.

[9] L. Harnefors, "Modeling of Three-Phase Dynamic Systems Using Complex Transfer Functions and Transfer Matrices," in IEEE Transactions on Industrial Electronics, vol. 54, no. 4, pp. 2239-2248, Aug. 2007.